

# IMPROVING THE PERFORMANCE OF TUFTED COMPOSITE SANDWICH STRUCTURES

Jamie W. Hartley\*, Matthew Dyson and Carwyn Ward

Advanced Composites Centre for Innovation and Science (ACCIS)  
University of Bristol, Bristol, UK

\*E-mail: jamie.hartley@bristol.ac.uk, Phone: +44 (0) 7584575593

**Keywords:** Crashworthiness, Edgewise Compression, Sandwich Structures, Through-thickness Reinforcement, Tufting

## ABSTRACT

A novel test method has been developed to test the contribution of the tuft drift mechanism observed in tufted sandwich structures under crushing loads. A test fixture has been produced capable of replicating the mechanism for a range of tuft configurations. Tests were carried out, looking at the number, alignment and spacing of tufts within the foam, and their effects on the load and energy absorption of the material. Results of the tests showed single tufts behaving in a consistent manner, but multiple tuft configurations were harder to control. An increased load, and hence energy absorption was observed with increasing numbers of tufts, however this effect diminished if interactions between the tufts did not take place. Future work would look to improve the test method, and ensure that the alignment of tufts could be better controlled to ensure a more accurate representation of failure mechanisms observed in larger test panels.

## 1 INTRODUCTION

Due to the increasing legislative pressure on Automotive manufacturers to reduce emissions and increase fuel efficiency [1], there is a shift within the industry towards the use of lightweight fibre-reinforced polymer (FRP) composite structures [2]. Sandwich structures are an effective way of increasing structural stiffness whilst maintaining low weight, and have the added potential of vibration damping and noise insulation [3], a key requirement for use in automotive vehicles.

For any material or structure to be considered for an automotive application, it must be capable of protecting the occupants from the large forces experienced during a crash. One of the most difficult cases to design for is an edgewise impact from a narrow roadside object such as a lamppost or utility pole, as there is little room to dissipate the energy of the concentrated impact. Whilst the use of FRPs is potentially a lightweight design solution due to the brittle failure of the material potentially absorbing more energy than current metallic structures [4], the use of FRPs within safety systems is currently limited to the high performance and motorsport sectors. For sandwich structures in particular, an inherent weakness at the interface between skin and core can lead to a catastrophic unstable collapse of the structure, under an edgewise impact load, which is not an efficient energy absorbing mechanism [5].

Amongst other through-thickness reinforcement methods [6,7], tufting has recently stood out as a technique for reinforcing the weak interface of a sandwich structure, and improving the failure behaviour, by mechanically tying the skins and core together. Tufting originated as an ancient carpet manufacturing technology but has recently gained popularity as a method of through-thickness reinforcement for composite materials. Unlike more traditional stitching methods, tufting uses a single threaded needle to insert a reinforcing thread, and relies on friction alone to hold the reinforcement in place [8]. As only a single needle is used, the surface features of the reinforcement are not symmetric, with a seam of thread formed on the insertion side, and a loop of thread formed on the back face. The advantages of tufting over more conventional methods stem from the need for only one needle. A single needle means access is only needed to one side of the preform, increasing the allowable

manufacturing complexity. There is also less damage to the preform from the use of multiple needle insertions [9]. Finally, the use of friction to hold the reinforcement in place means that reduced crimping of the fabric takes place, compared to traditional stitching methods, which better maintains the in-plane mechanical properties of the final cured part [10,11]. However, a limited understanding of the technology when applied to sandwich structures, particularly ensuring control of the manufacturing process [9], has up to now restricted its use.

Over the past decade, several researchers have explored and demonstrated the advantages of tufting in both monolithic and sandwich structures under a range of design cases [12–15]. More recently, a study of particular interest by Blok et al. [16] demonstrated the potential of tufts to improve the crashworthiness of sandwich structures under edgewise loading. They found that the use of tufts restrained the separation of skin and core, resulting in increased fracture of the facesheets, and a significantly increased amount of energy absorbed. Whilst these performance improvements are a positive step forward for the technology, a better understanding of the mechanism is required to be able to make informed design choices in the future. An investigation by Hartley et al. [17] explored the ‘unit cell’ of a tufted panel, focusing on the effect of the tuft length and local density on mechanical performance. Whilst it was seen that tuft length had very little effect on performance it was found that the tuft thickness and local density, did. From further analysis, it was observed that the primary failure mechanism of the tuft was separation at the skin-core interface. The process of inserting the tufting needle into the preform leaves a complimentary void within the foam core. During the subsequent infusion, these voids fill with resin, which on curing leaves an array of rigid columns within the core. After the tufts separated, these resin columns advanced through the core, resulting in an internal crushing mechanism of the foam.

### 1.1 Detailed failure of tufted sandwich panels

A recent study carried out by the authors [18] tested scaled (~50 mm) tufted sandwich coupons under edgewise compression in order to capture the local failure modes exhibited by the structure and the tufts within. Tested coupons displayed an edgewise crushing failure featuring folding and delamination of the skin laminates, as well as crushing of the foam core. Aside from the overall global failure mechanism of the coupon, the internal failure of the tufts was also successfully captured. As discussed previously, the tufts were seen to fail at the skin-core interface before sliding through the core as crushing of the coupon progressed. When the compression limit of the dividing foam region between two tufts was reached, the tufts would stack and begin to slide together. A time-lapse of the crushing mechanism featuring column drift is shown in Figure 1. Alongside the column drift mechanism observed, several of the local failure mechanisms that occur around this process were also identified. These included fracturing within the skins, compressive failure of the foam core and rupturing of the resin columns. In several cases the tufting threads were also observed to have been pulled out of the resin columns.

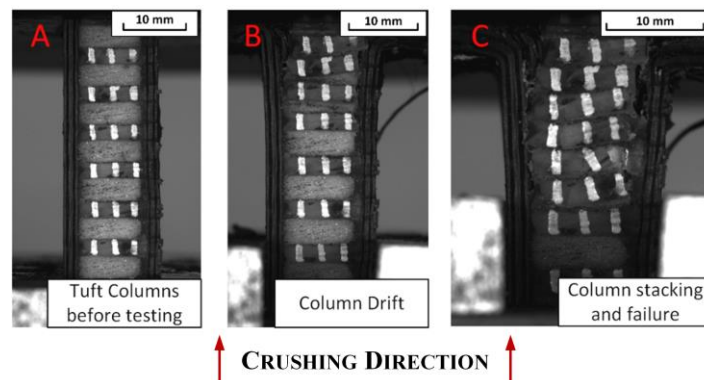


Figure 1: Progressive crushing mechanism observed in tufted sandwich structures. **A)** Tuft positioning before testing. **B)** Separation and subsequent ‘drifting’ of tufts. **C)** Stacking and failure of tuft resin columns [18].

A summary of the test results from these experiments is shown in Table 1. A typical metric for measuring the performance of a structure or material for crashworthiness is the specific energy absorption (SEA) [19]. The SEA is given by:

$$SEA = \frac{W}{\rho A \delta} = \frac{\int_0^{\delta} F dx}{\rho A \delta} \quad (1)$$

Where  $W$  is the energy absorbed by the crushing of the material, and  $\rho A \delta$  is the mass of material crushed. From the results in Table 1, generally the tufted coupons displayed a higher relative energy absorption, because of the more stable and efficient failure mechanism that takes place in tufted sandwich structures.

Table 1: Summary of test results recorded from sandwich crushing tests. *Grey shading highlights samples that failed by unstable collapse.*

Group	Sample	Total Energy Absorbed	SEA
-	-	(kJ)	(kJ/kg)
Reference	R1	0.50	98.7
	R2	0.11	41.3
	R3	0.12	23.2
Short – 40 mm	1	0.31	48.4
	2	0.22	42.5
	3	0.36	53.9
Medium – 50 mm	4	0.24	41.0
	5	0.45	53.4
	6	0.30	36.3
Long – 60 mm	7	0.34	41.1
	8	0.17	17.3
	9	0.62	54.8

Whilst the performance improvements from tufting under this load case have been shown, it is not yet understood how the failure mechanisms occurring contribute to the energy absorption within the structure. With this information, better design choices could be made when deciding on the design, location and spacing of the tufts within the structure. Locating tufts at the correct areas would reduce the number used, allowing for a reduction in the overall processing time of the structural preform, and a reduced mass of the final structure. This could as well lead to potential modifications in the tufting process, to control resin intrusion into some areas of the structure and thus reduce the mass further. In this paper, a novel mechanical testing technique will be developed to investigate one of these failure mechanisms in detail. The chosen behaviour of focus is the drifting mechanism of the tufts through the core. The test will simulate both the failure of the surrounding core material as the tuft progresses, as well as the interaction between neighbouring tufts during the process.

## 2 METHODOLOGY

Several test approaches were evaluated to choose the most suitable method of simulating the drifting of tufts within the core. An initial trial was carried out by testing a sheet of foam in edgewise compression, the closest possible representation of previously tested sandwich coupons. However, the relatively low thickness and stiffness of the foam sheet was such that it was too unstable under load, and would fail by buckling (Figure 2) and not crushing as desired.

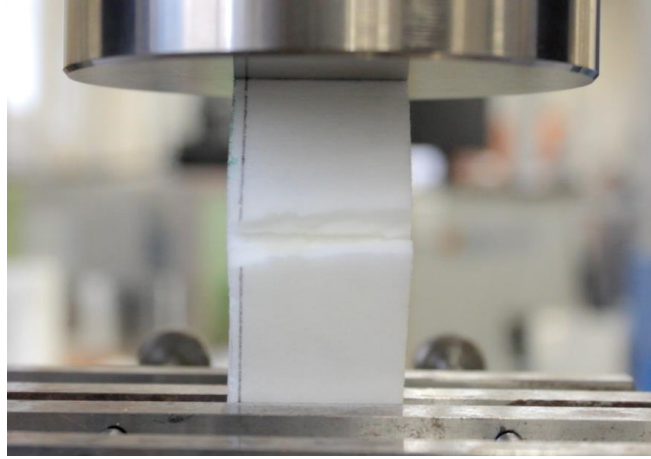


Figure 2: Buckling of foam sheet under direct edgewise compression loading.

A second trial was carried out, loading the foam in a flatwise direction, to increase its crushing stability. Short pins were cut to 10 mm from lengths of steel rod (Figure 3) and placed on the foam to simulate the presence of the tufts. Whilst movement of the rod through the foam was observed, the relatively low thickness resulted in a very short termination time for the test, and the inability to use multiple tufts in one specimen. The large load required to crush the foam also meant that it was very difficult to observe the changes affected by the insertion of the pins.



Figure 3: A comparison of a tufted resin column (left) and the steel pin used (right).

For the final chosen test configuration it was decided to pull the pins through the core in a tensile manner, instead of relying on compressing the foam core. To achieve this, a test fixture was designed and produced, capable of supporting and applying load to multiple pins embedded within the foam core. The design of the test fixture is shown in Figure 4. The design of the fixture allows for the insertion of multiple pins, to simulate different tufting configurations. The spacing between each hole was 6 mm, to match the minimum spacing used in previous testing [16,17]. The fixture was laser cut from transparent Perspex sheets of 10 mm thick, to allow visual tracking of the pins as they moved through the foam.

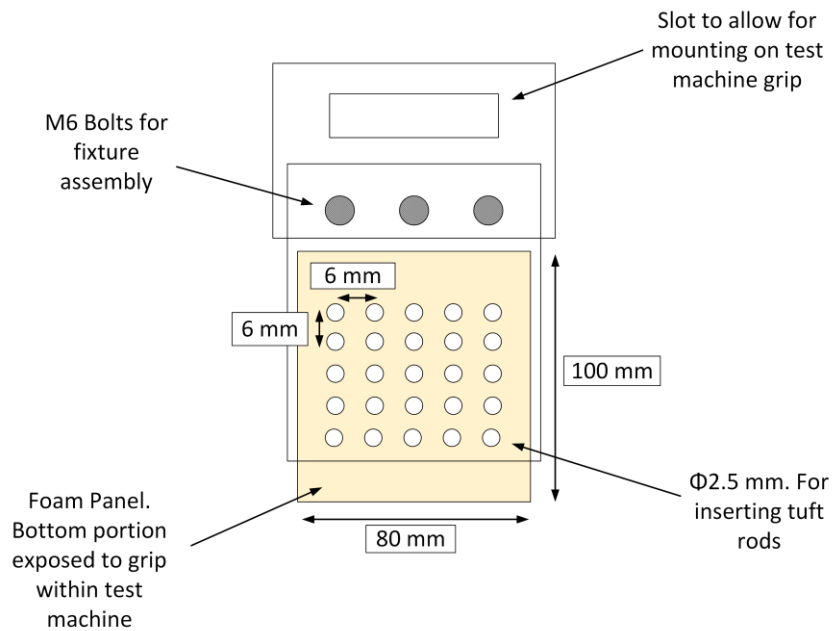


Figure 4: Schematic of test fixture used.

Load was applied to the specimen using a Shimadzu desktop electromechanical test machine, with a 1kN load cell. The upper part of the fixture featured a slot for the upper stage grip of the test machine to slot into, whilst at the bottom a section of the foam was left exposed and was mounted in the lower test grip, as shown in Figure 5. Sand paper (P60 grit) was used to increase the friction between sample and loading grip, and avoid slipping. The loading rate applied was 4 mm/min. An Imetrum<sup>®</sup> video gauge system was used for visual tracking of the test. This camera system was able to track the movement of individual pixels within an image, thus following the movement of the pins as they moved through the foam. The system also allowed video playback of test, allowing failure behaviour to be viewed and identified.

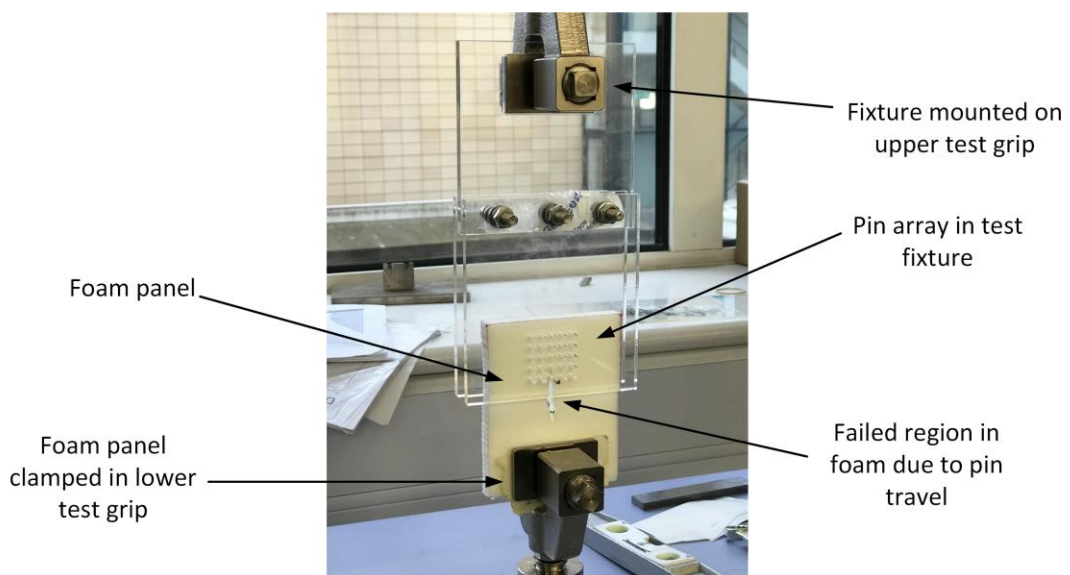


Figure 5: Setup of test fixture on Shimadzu test machine.

For the materials selection, a Rohacell<sup>®</sup> 110 IG-F closed-cell foam by Evonik (110 kg/m<sup>3</sup>) was chosen for the foam, to match previous testing [16,17]. A rigid steel rod of 2.3 mm diameter was chosen to simulate the tufts (Figure 3). This choice was made to avoid any deformation or fracture of

the columns taking place during testing. As can be seen from the image, there are slight differences in geometry and dimensions of the two columns. Whilst the tufting needle is smooth and the dimensions are fixed, the resin infusion process through the foam core leaves a rough outer surface. The rigid steel rod used is therefore an idealised case.

To insert the pins, a small pin hammer was used to gently knock the pins into the foam. To apply loading directly to the pins, those that were required to be loaded were left deliberately longer than the through thickness dimension of the foam and test fixture, in order to allow the test fixture to pull the pin as it moved. To simulate collisions between the loaded pins and the passive unloaded pins it was necessary to cut these slightly shorter than the foam thickness so they could move freely through the material. A total of nine configurations were tested, with varying locations and numbers of pins inserted to simulate different tuft configurations. Initially a baseline set of data was created, using a single, centrally positioned pin. Further configurations were created to explore the effects of multiple pins, either loaded in parallel or in line with each other, as well as two-dimensional pin arrays. A summary of the test configurations and their naming conventions is given in Figure 6. Those pins that are loaded and those that are not are highlighted in the figure.

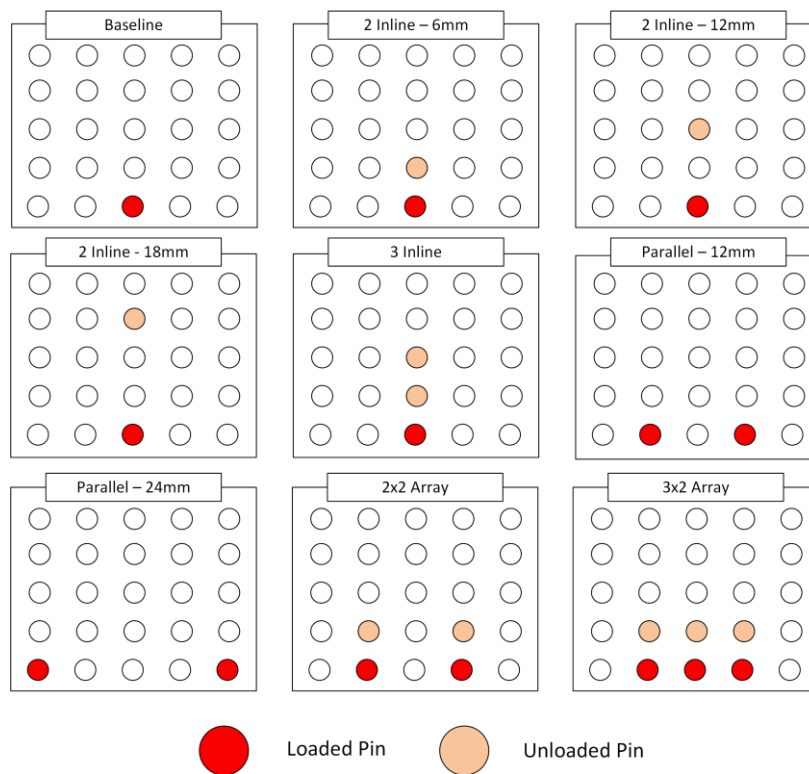


Figure 6: Positioning of loaded and unloaded for each test configuration considered.

### 3 RESULTS AND DISCUSSION

#### 3.1 Single Pin - Baseline

The results of the baseline tests, featuring a single central rod are shown in Figure 7. The load trace shows an initial sharp increase in load up to the point of failure of the foam. Beyond this point the rod begins to slide through the foam sheet (Figure 9-A). As the rod slides, it compresses material in its path, resulting in a gradual increase in load as the test progressed. Of the four samples tested, each showed a very similar trend in loading, although some variation between the peak loads were observed. This is potentially due to the insertion method of the rod, as tapping the pin against the foam could have led to cracks and potential weak spots in the material. This would be inconsistent between samples and thus result in slight variations in load.

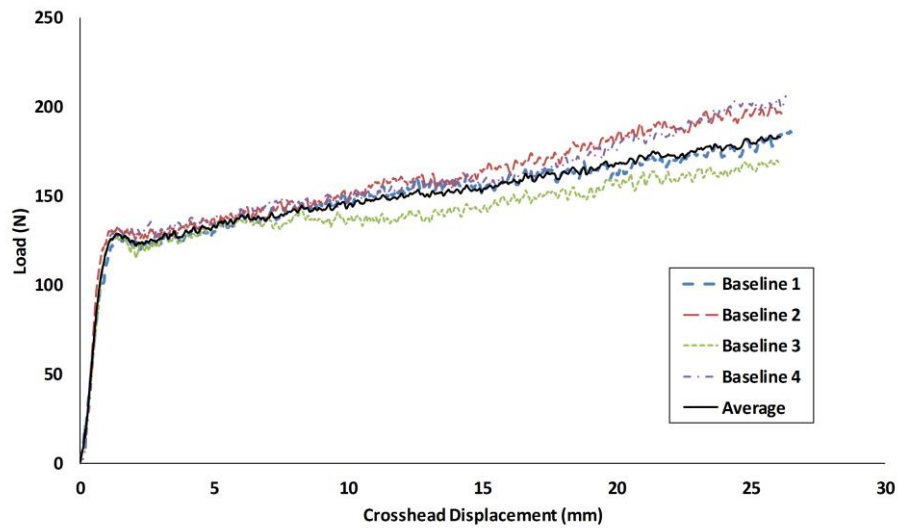


Figure 7: Load-displacement results for baseline tests.

### 3.2 Multiple Pins

Following on from the single pin baseline tests, configurations featuring multiple tufts were tested to explore the interactions between the tufts. Two placement strategies were explored, firstly by loading the pins in parallel, followed by lining the pins up in the same vertical plane. These were finally combined together to give a two-dimensional array of pins.

#### 3.2.1 Parallel

The results of the parallel tests are shown in Figure 8. Due to the consistency between results only two test samples were used, with a varied gap size between them. It can be seen from the results that the load is approximately double the baseline as a result of loading two pins in parallel, due to the requirement to crush the foam in two different locations. Doubling the gap between the pins had no effect on the load. Another noticeable difference when compared to the baseline was the smooth transition from the initial rapid load increase phase to the rod moving stage. This may be due to the increased number of pins stopping rotation of the sample, and thus eliminating any sudden changes in load.

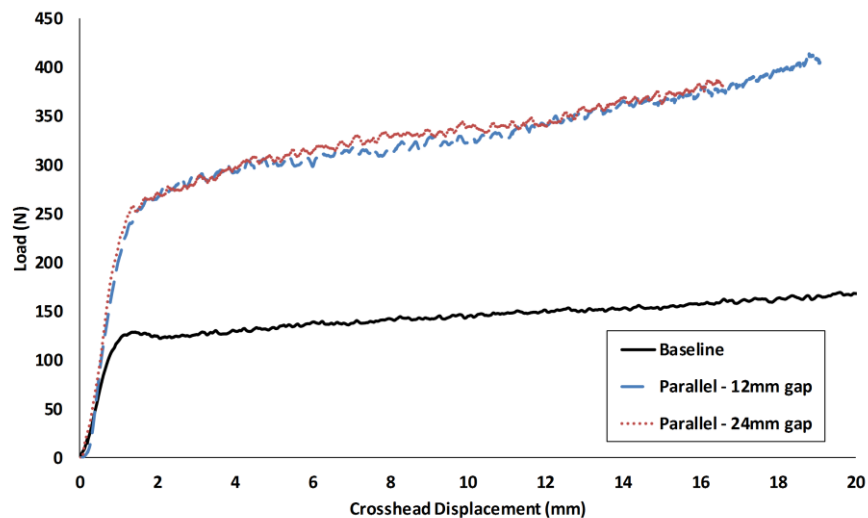


Figure 8: Load-displacement results for parallel pin configuration tests.

### 3.2.2 Inline

For the inline tests, the pins were placed in a straight line along the centre of the foam panel. Following the load trace in Figure 10, the load in each case increased sharply at the same rate as the baseline until the foam around the pin began to fail. From this point onwards, the load of each test configuration generally increased, although with significant fluctuations in the load. For the 2 pin configurations, there is a secondary increase in load as the loaded and unloaded pins begin to collide with each other, and the unloaded pin is driven through the foam Figure 9-B. From this point onwards the load remains steady, above the baseline load curve, but tends to return to the baseline level as the test progressed. The secondary rise in load changed with pin spacing, with the 6 mm occurring earliest, followed by the 18 mm and then the 12 mm. The 3 pin configurations showed a similar trend, but with two noticeable load increases corresponding to the two pin interactions taking place. It was observed during testing that in a number of cases the loaded pins would slide around the unloaded pins, as seen in Figure 9-C. Similar behaviour has been observed in metallic structures, where compressive residual stress around pins can cause redirection of fatigue cracks [20]. However, it is not clear at this stage if this behaviour is occurring here. It was apparent that this occurred more often with larger pin spacing, which implies that the larger the gap, the harder it is to control the pin movement and collisions. As a result of this, the shortest gap (6 mm) resulted in the largest consistent increase in load, as the unloaded pin was pushed for a much longer distance.

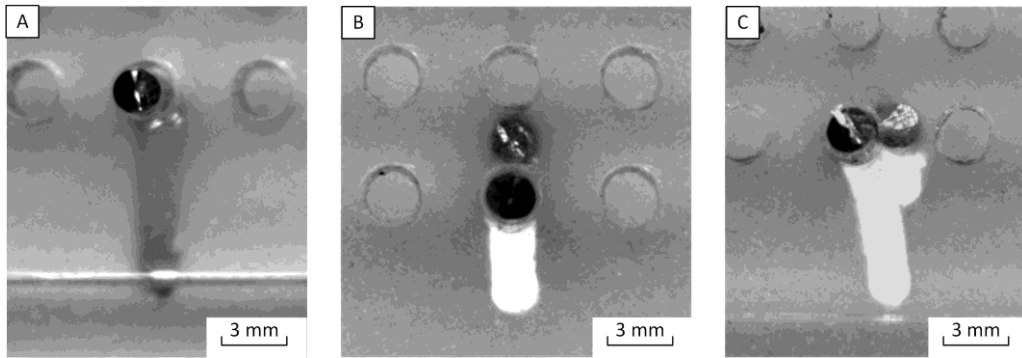


Figure 9: Sliding mechanism of pins through foam. **A)** Single pin baseline. **B)** Two pins inline moving together. **C)** Two pins inline, loaded pin realigning to avoid unloaded pin ahead.

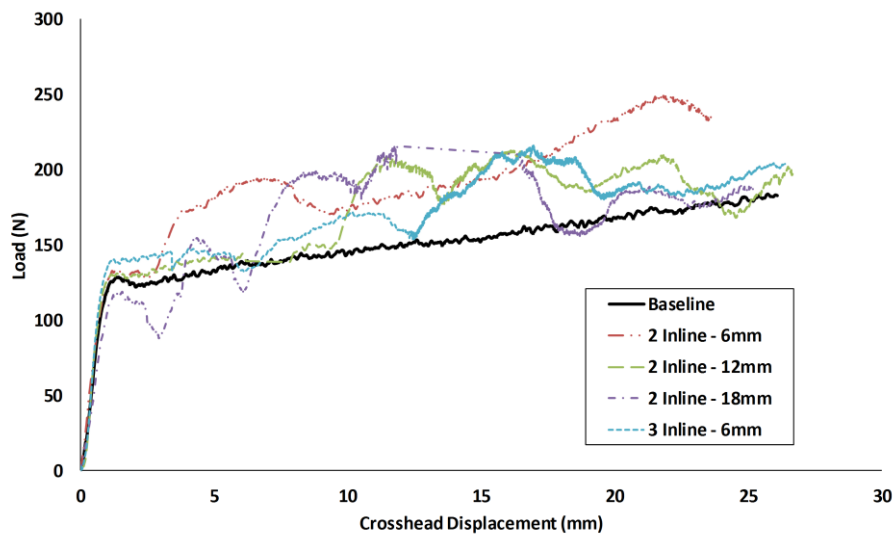


Figure 10: Load-displacement results for inline pin placement tests.

### 3.2.3 Array

By increasing the number of pins in both directions the load trace is observed to increase concurrently. As with each of the test configurations discussed previously, the initial loading phase follows a sharp increase in load before levelling off. The 2x2 array showed a slight drop in load after this point, followed by a load recovery at around 4 mm of displacement. The sustained load from this point is approximately 20% higher than the 2 pin parallel configuration. There is a slight increase and peak of the load at 17mm of displacement, as a result of the loaded pins moving past the unloaded pins. The 3x2 array showed a much greater increase in load, as a result of the 3 loaded pins. As with the 2x2 array, there is a slight drop in load after the initial rise, followed by a steady increase. After a short test displacement of 7 mm, cracks began to appear around the loaded pins which grew rapidly and fractured the foam. At this point the test was aborted and was not continued to due to the foam being unable to handle the excessive loading conditions.

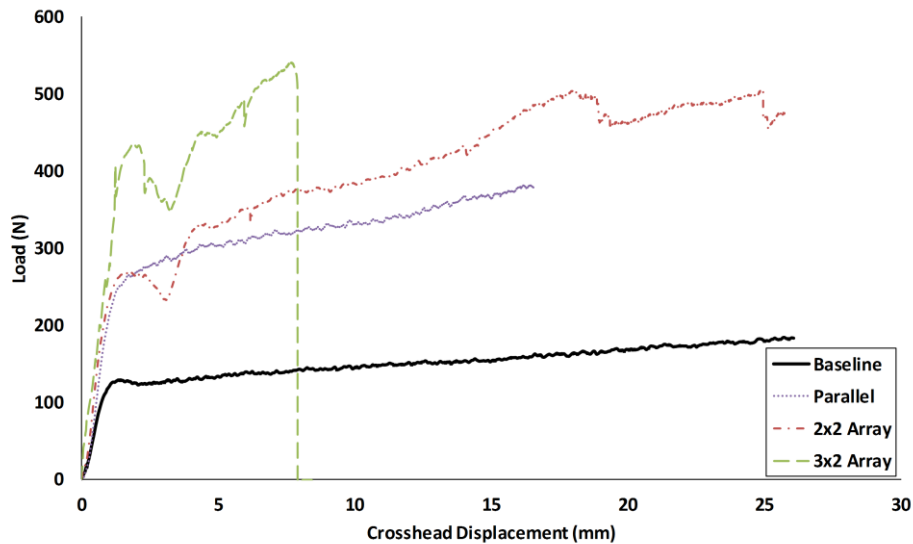


Figure 11: Load-displacement results for array pin placement results.

### 3.3 Energy Absorption

The specific energy absorbed during the tests was calculated for each sample by accounting for the mass of foam crushed in the path of the loaded pins. As can be seen from the results in Table 2, the efficiency of energy absorption generally increased with increasing numbers of pins in the loading direction. The additional work required by the loaded pin to compress the foam surrounding the next pin and then the work required to move that pin meant that energy absorption was generally higher for each configuration. Another point to note is that magnitude of the energy increase and the consistency between results. The variation between results also increased as the gap space increased, which suggests there is greater margin for error for the loaded pin to move out of alignment as it travels through the foam.

Compared to the values shown in Table 1, the absolute energy absorbed during these tests was relatively small, roughly two orders of magnitude lower than the full sandwich coupons tested previously [18]. This suggests that for the tuft drifting mechanism to be of any benefit to the overall crushing performance then the tuft density within the sandwich panel should be high. However testing has shown that collisions between tufts on a small scale can still add significant improvements to the energy absorption of a single tuft. If these collisions could be controlled, by forcing the path of the tuft during failure, a substantial increase to the energy absorbing efficiency of the structure could be made.

Table 2: Averaged energy absorption results for each pin configuration tested.

Type	Samples Tested	Average SEA per loaded pin (kJ/kg)	% Change	CV (%)
Baseline	4	59.8	-	4.50
2 pins inline - 6mm	5	77.7	30%	4.55
2 pins inline - 12mm	3	68.6	15%	11.3
2 pins inline - 18mm	3	66.5	11%	6.39
3 pins inline - 6mm	4	67.9	14%	6.04
2 pins parallel	2	62.4	4%	0.78
2x2 array	3	79.4	33%	6.19
3x2 array	1	50.4	-16%	0

#### 4 TEST METHOD DEVELOPMENTS

Whilst the test method outline in this work has successfully captured data from the tuft drift and collision mechanism during crushing, there are still aspects to the test that could be improved. The first of these is to ensure a clean insertion method for placing the pin within the foam panel prior to testing. The current method using a small hammer gives rise to the possibility of damage forming within the foam, as well as the potential for the pin to not enter the foam at the correct angle. An improved method would see the use of a linear actuator with an actual tufting needle fitted to ensure a clean hole through which to insert the pin. The second step required would be to ensure no rotation of the foam panel, or transverse motion of the pin is allowed, to ensure clean contact and continued stacking between the loaded and unloaded pins.

#### 5 CONCLUSIONS

A novel test method has been developed and demonstrated to represent the behaviour of tufts within a sandwich structure during crushing. A metallic pin was used to represent a tuft and inserted into a foam panel. The pin was loaded in tension to force it to slide through the foam. Consistent loading results were observed for a single pin before the test was expanded to consider multiple pins in different configurations. It was observed that the load required to drive the pin was directly proportional to the number of parallel pins being loaded. Pins placed in line with each other also showed an increase in load, particularly when the pins successfully stacked and moved together. This stacking behaviour was inconsistent, and was hard to achieve the greater the distance between pins, or the larger the numbers used. Future developments may need to focus on ensuring the pins travel in one fixed direction without realigning, as well as an improved insertion technique to ensure flaws are not present within the foam before testing.

#### ACKNOWLEDGEMENTS

This work was supported by the Engineering and Physical Sciences Research Council through the EPSRC Centre for Doctoral Training in Advanced Composites for Innovation and Science (Grant: EP/G036772/1) and the EPSRC Centre for Innovative Manufacturing in Composites (CIMComp) (Grant: EP/IO33513/1).

#### REFERENCES

- [1] European Parliament and Council of the European Union. Official Journal of the European Union 2009;55.
- [2] Tucker N, Lindsey K. An Introduction to Automotive Composites. Rapra Technology Ltd; 2002.
- [3] Hara D, Özgen GO. Investigation of Weight Reduction of Automotive Body Structures with the Use of Sandwich Materials. Trans Res Procedia 2016;14:1013–20.

- [4] Jacob GC, Fellers JF, Starbuck JM. Energy Absorption in Polymer Composite Materials for Automotive Crashworthiness. *J Compos Mater* 2008;36:813–38.
- [5] Mamalis AG, Manolakos DE, Ioannidis MB, Papapostolou DP. On the crushing response of composite sandwich panels subjected to edgewise compression: Experimental. *Compos Struct* 2005;71:246–57.
- [6] Nanayakkara AM, Feih S, Mouritz AP. Improving the fracture resistance of sandwich composite T-joints by z-pinning. *Compos Struct* 2013;96:207–15.
- [7] Aktas A, Potluri P, Porat I. Development of through-thickness reinforcement in advanced composites incorporating rigid cellular foams. *Appl Compos Mater* 2013;20:553–68.
- [8] Dell'Anno G, Treiber JWG, Partridge IK. Manufacturing of composite parts reinforced through-thickness by tufting. *Robot Comput Integr Manuf* 2016;37:262–72.
- [9] Tan G, Hartley J, Withers E, Kratz J. Towards the Development of an Instrumented Test Bed for Tufting Visualisation. *SAMPE Eur. Conf.*, Amiens: 2015.
- [10] Dell'Anno G, Cartié DD, Partridge IK, Rezaei A. Exploring mechanical property balance in tufted carbon fabric/epoxy composites. *Compos Part A Appl Sci Manuf* 2007;38:2366–73.
- [11] Treiber JWG. Performance of tufted carbon fibre/epoxy composites. Cranfield University, 2011.
- [12] Liu L, Zhang T, Wang P, Legrand X, Soulat D. Influence of the tufting yarns on formability of tufted 3-Dimensional composite reinforcement. *Compos Part A Appl Sci Manuf* 2015;78:403–11.
- [13] Cartié DDR, Dell'Anno G, Poulin E, Partridge IK. 3D reinforcement of stiffener-to-skin T-joints by Z-pinning and tufting. *Eng Fract Mech* 2006;73:2532–40.
- [14] Deconinck P, Capelle J, Bouchart V, Chevrier P, Ravailier F. Delamination propagation analysis in tufted carbon fibre-reinforced plastic composites subjected to high-velocity impact. *J Reinf Plast Compos* 2014;33:1353–63.
- [15] Henao A, Carrera M, Miravete A, Castejón L. Mechanical performance of through-thickness tufted sandwich structures. *Compos Struct* 2010;92:2052–9.
- [16] Blok L, Kratz J, Lukaszewicz D, Hesse S, Ward C, Kassapoglou C. Improvement of the in-plane crushing response of CFRP sandwich panels by through-thickness reinforcements. *Compos Struct* 2017;161:15–22.
- [17] Hartley JW, Kratz J, Ward C, Partridge IK. Effect of tufting density and loop length on the crushing behaviour of tufted sandwich specimens. *Compos Part B Eng* 2017;112:49–56.
- [18] Hartley JW, Tse G, Kratz J, Ward C, Partridge IK. Column interaction in tufted sandwich structures under edgewise loading. *ECCM17 – 17th Eur. Conf. Compos. Mater.*, 2016.
- [19] Elmarakbi A. *Advanced Composite Materials for Automotive Applications: Structural Integrity and Crashworthiness*. Chichester, UK: John Wiley & Sons Ltd; 2013.
- [20] Makabe C, Murdani A, Kuniyoshi K, Irei Y, Saimoto A. Crack-growth arrest by redirecting crack growth by drilling stop holes and inserting pins into them. *Eng Fail Anal* 2009;16:475–83.